



Contents lists available at ScienceDirect

## Arabian Journal of Chemistry

journal homepage: [www.ksu.edu.sa](http://www.ksu.edu.sa)

Original article

## Antioxidant properties of acteoside against biological systems: Hemoglobin and cardiomyocyte as potential models

Xiaoqiong Zhang<sup>a,1</sup>, Shanshan Cui<sup>b,1</sup>, Yugang Zu<sup>c,\*</sup>, Cuina Feng<sup>c,\*</sup><sup>a</sup> Department of Cardiovascular Medicine, Baoding Second Hospital, Baoding 071000, China<sup>b</sup> Department of General Medicine, Affiliated Hospital of Hebei University, Baoding 071000, China<sup>c</sup> Department of Cardiovascular Medicine, Affiliated Hospital of Hebei University, Baoding 071000, China

## ARTICLE INFO

## Keywords:

Acteoside

Oxidative stress

Hemoglobin structural changes

Cardiomyocyte

## ABSTRACT

Oxidative stress has been shown to be the main cause of protein denaturation and cell death. However, the exact mechanism of antioxidants against oxidative stress-mediated protein damage and cell cytotoxicity remains largely unknown. Therefore, in this paper, the protective effects of acteoside against H<sub>2</sub>O<sub>2</sub>-induced hemoglobin structural changes and cardiomyocyte toxicity as models were determined by different techniques. Fluorescence quenching as well as molecular docking simulation studies showed that acteoside potentially interacted with hemoglobin in a one: one binding mode mediated mainly by the involvement of hydrophobic forces. It was also shown that H<sub>2</sub>O<sub>2</sub> caused significant changes in the structure of hemoglobin as well as heme degradation, reversed by acteoside. Additionally, UV-visible studies exhibited that acteoside decreased the generation of methemoglobin triggered by H<sub>2</sub>O<sub>2</sub>. Cellular assays displayed that acteoside could mitigate the cardiomyocyte toxicity induced by H<sub>2</sub>O<sub>2</sub> through regulation of LDH release, generation of reactive oxygen species (ROS) and 3,4-methylenedioxyamphetamine (MDA), mitochondrial membrane potential (MMP) collapse, as well as superoxide dismutase (SOD), catalase (CAT), caspase-9, and caspase-3 activities. In conclusion, acteoside may hold great promise for the control of protein-related disorders as well as cardiovascular diseases.

## 1. Introduction

It has been established that oxidative damage to biomolecules and cells plays a critical role in the stimulation of many human diseases (de Araújo, Martins et al. 2016). The imbalance of the oxidants and antioxidant signaling pathways could result in oxidative stress-related diseases (Remigante and Morabito, 2022). We still don't fully understand how reactive oxygen species (ROS) can cause oxidative damage at the biomolecular and cellular levels. For example, oxidative damage of protein could be a main reason for the stimulation of aging, and several other diseases (Liguori, Russo et al. 2018). Protein and cell oxidative damage leads to structural/functional disruption as well as apoptosis, respectively, which become the most common factors for the onset of different human diseases.

Hemoglobin as a crucial circulatory plasma protein serves as an oxygen carrier protein. Oxidative stress could directly affect the oxidative state of hemoglobin which subsequently results in a significant change in the hemoglobin structure and function (Reeder and Wilson, 2005,

Rasheed, Alharbi et al. 2022). For example, Rashhed et al. reported that oxidative stress could result in extensive damage to hemoglobin structure evidenced by tryptophan fluorescence quenching, hydrophobicity, and carbonylation measurements (Rasheed, Alharbi et al. 2022). However, the efforts to mitigate the oxidative damage to hemoglobin are still largely unexplored.

In the heart, although ROS could play a key role in cell homeostasis mediated by regulating cell growth and differentiation, excessive ROS might lead to cellular and molecular malfunctions, ultimately causing cardiac dysfunction. ROS overproduction might stimulate cardiomyocyte apoptosis, myocardial inflammation and impaired cardiomyocyte proliferation (Zhang, Li et al., 2018, Wu, Guo et al. 2022a).

Therefore, it may be worthwhile to explore how antioxidant therapies may affect the control of oxidative stress-related cell and protein damage.

Acteoside (verbascoside or kusagin, C<sub>29</sub>H<sub>36</sub>O<sub>15</sub>, [ $\beta$ -(3,4-dihydroxyphenylethyl)-O- $\alpha$ -L-rhamnopyranosyl-(1  $\rightarrow$  3)- $\beta$ -D-(4-O-caffeoyl)-glucopyranoside]) as a phenylethanoid glycoside has been highly isolated

\* Corresponding authors at: NO.212, Yuhua East Road, Baoding 071000, Hebei Province, China.

E-mail addresses: [zhangxiaoqiong@163.com](mailto:zhangxiaoqiong@163.com) (Y. Zu), [fengcuina1@163.com](mailto:fengcuina1@163.com) (C. Feng).<sup>1</sup> Contributed equally to this study.<https://doi.org/10.1016/j.arabjc.2024.105630>

Received 3 October 2023; Accepted 11 January 2024

Available online 17 January 2024

1878-5352/© 2024 The Authors. Published by Elsevier B.V. on behalf of King Saud University. This is an open access article under the CC BY-NC-ND license (<http://creativecommons.org/licenses/by-nc-nd/4.0/>).

from dicotyledonous plants (Xiao, Ren et al. 2022). Thanks to its polyphenolic structure, acteoside shows potential antioxidant properties and could potentially interact with proteins and cells in the human body. Therefore, acteoside as a promising bioactive compound with different pharmacological activities (Xiao, Ren et al. 2022) could receive great attention in the development of antioxidant agents. Given these facts, we may hypothesize that acteoside serves as a potential antioxidant against oxidative stress-induced protein and cell reshaping. To address this hypothesis, we chose human hemoglobin and cardiomyocyte as studied models and incubated them with hydrogen peroxide ( $H_2O_2$ ) in the absence or presence of acteoside. The antioxidant potential of acteoside was analyzed by different spectroscopy, and cellular and molecular assays. Our promising data may have crucial implications for the development of new therapeutic approaches for ROS-related human disorders.

## 2. Materials and methods

### 2.1. Materials

Human hemoglobin (CAS No.: 9008-02-0), thiazolyl blue tetrazolium bromide (MTT),  $H_2O_2$  in a 30 % (w/w) solution, and acteoside (verbascoside or kusagin, CAS No.: 61276-17-3) were purchased from Sigma-Aldrich (USA). All other materials were of analytical grade.

### 2.2. Sample preparation

The human hemoglobin solution was prepared in phosphate buffer (10 mM, pH = 7.4, 100 mM NaCl) containing 100 mM NaCl, while the acteoside solution was prepared in ethanol and diluted in phosphate buffer (10 mM, pH = 7.4, 100 mM NaCl) or cell culture medium.

Also, hemoglobin solutions at a concentration of 80  $\mu$ M were treated with  $H_2O_2$  at molar ratios of heme to peroxide of 1:0 and 1:5, while after 1 h  $H_2O_2$  was removed from the samples through buffer exchanging with equal volumes of phosphate buffer (10 mM, pH = 7.4, 100 mM NaCl), using 30-kDa cut-off centrifuge tubes as reported previously (Jia, Buehler et al. 2007). To measure the protective effects of acteoside against oxidative stress-protein damage, hemoglobin samples were co-treated with acteoside at molar ratios of protein to acteoside of 1:0 and 1:1, followed by the addition of  $H_2O_2$ .

### 2.3. Fluorescence quenching studies

The fluorescence spectra were recorded on a spectrofluorometer (F-4500, Hitachi, Japan). Both excitation and emission slit widths were fixed at 5 nm. The temperature for the fluorescence quenching studies was set to 298 K, 308 K and 315 K by a water circulator. A 3.0 mL solution of hemoglobin with a concentration of 4.00  $\mu$ M was added by successive titrations of acteoside solution, where acteoside concentrations varied from 4 to 50  $\mu$ M. Fluorescence spectra were then recorded in the range of 300–490 nm, while the excitation wavelength was set to 280 nm. Reported data were corrected against the inter-filter effects of hemoglobin and acteoside, according to the mathematical procedures reported previously (Basu and Kumar, 2016).

Also, the protective effects of acteoside on  $H_2O_2$ -induced fluorescence quenching of hemoglobin were measured by fluorescence spectroscopy study. The aliquots of protein samples (80  $\mu$ M) incubated with  $H_2O_2$  (molar ratios of heme to peroxide of 1:5) for 1 h in the absence and presence of acteoside (molar ratios of protein to acteoside of 1:1) were withdrawn and used for protein quenching study.

### 2.4. Molecular docking study

The 3D structure of human hemoglobin was obtained from the Protein Data Bank (PDB: 4ROL). acteoside structure was obtained in sdf format from PubChem with PubChem CID: 354009. AutoDock Vina was

used to carry out molecular docking simulations. Cavity-detection guided blind docking was used to detect potential binding sites. The grid parameters were 28, 28, 28 centralized at 7, 8, 47 Å. The exhaustiveness and grid spacing were set as default. Post-docking analysis was performed using BIOVIA Discovery Studio Visualizer.

### 2.5. Circular dichroism (CD) spectroscopy

Changes in the secondary structure and heme microenvironment of hemoglobin were measured using a CD spectrometer (Jasco J-1500, Japan) equipped with a 0.2 cm quartz cuvette. The aliquots of protein samples (80  $\mu$ M) incubated with  $H_2O_2$  (molar ratios of heme to peroxide of 1:5) for 1 h without or with acteoside (molar ratios of protein to acteoside of 1:1) were withdrawn and used for CD study. The CD spectra were read at ambient temperature in the range of 200–260 nm. Also, ellipticity changes of hemoglobin were monitored in the Soret region (420 nm). Each spectrum was corrected against acteoside and buffer signals.

### 2.6. UV-Vis spectral measurement

The UV-Vis spectra of aliquots of protein samples (80  $\mu$ M) incubated with  $H_2O_2$  (molar ratios of heme to peroxide of 1:5) for 1 h without or with acteoside (molar ratios of protein to acteoside of 1:1) were withdrawn and used for detection of methemoglobin on a UV-Vis spectrophotometer (Cary 100, Varian Co, Australia) at ambient temperature. The amounts of methemoglobin were then determined from the UV spectra at 579 nm, 560 nm and 540 nm by the method of Benesch et al. reported previously (Benesch, Benesch et al., 1973).

### 2.7. Cell culture and treatment

The cardiac muscle cell line H9c2 obtained from Shanghai FuHeng Cell Center (Shanghai, China) was incubated at 37 °C in a 5 %  $CO_2$  humidified atmosphere in Dulbecco's modified Eagle's medium (DMEM, Gibco, Rockville, MD, USA) containing 10 % heat-inactivated fetal bovine serum (FBS, Gibco, Rockville, MD, USA), 100 Units/mL of penicillin, and 100  $\mu$ g/mL streptomycin (Gibco, Rockville, MD, USA). For all assays, the cells were cultured at appropriate densities relevant to the experimental design. H9c2 cells were pretreated with a fixed concentration (10  $\mu$ M) of acteoside for 12 h followed by washing and treatment with  $H_2O_2$  (400  $\mu$ M) for an additional 2 h (Shi, Geng et al. 2020).

### 2.8. Analysis of cell viability

Cell viability was determined using MTT assay. Briefly, H9c2 cardiomyocytes were seeded, pretreated with a fixed concentration (10  $\mu$ M) of acteoside 12 h, washed, and treated with 400  $\mu$ M  $H_2O_2$  for an additional 2 h. Then, 1 mg/mL MTT solution was added and the cells were incubated for 4 h at 37 °C. The supernatant was then gently removed and the cells were added by 150  $\mu$ L of DMSO. The absorbance of samples was read at 570 nm on a microplate reader (SpectraFluor, TECAN, Sunrise, Austria).

### 2.9. Assessment of LDH, MDA and antioxidant enzyme activities

The cells were seeded and pretreated with a fixed concentration (10  $\mu$ M) of acteoside for 12 h before the addition of  $H_2O_2$  (400  $\mu$ M) for an additional 2 h. The supernatant and the cardiomyocytes were then collected for measuring the LDH and MDA levels, as well as CAT and SOD activity with the corresponding detection kits (Abcam, Cambridge, MA, USA) according to the manufacturer's manual.

### 2.10. Measurement of intracellular reactive oxygen species (ROS)

To explore the protective effect of acteoside on the formation of intracellular ROS triggered by  $H_2O_2$ , cardiomyocytes were pretreated with a fixed concentration (10  $\mu M$ ) of acteoside for 12 h before the addition of  $H_2O_2$  (400  $\mu M$ ) for an additional 2 h. Then, the levels of intracellular ROS were measured using a ROS detection kit based on the manufacturer's manual (Abcam, Cambridge, MA, USA). Briefly, the cells were harvested, washed, centrifuged (1000 rpm for 5 min), resuspended in 500 mL ROS detection solution, incubated for 20 min at 37 °C, and analyzed by fluorimeter (BIOTEK-FLX800, USA) with excitation at 485 nm and emission at 520 nm.

### 2.11. Determination of mitochondrial membrane potential (MMP)

The levels of MMP were measured by the 5,5',6,6'-tetrachloro-1,1',3,3'-tetraethylbenzimidazolylcarbocyanine iodide (JC-1) dye (Gibco, Rockville, MD, USA) quantitatively as the total fluorescence was assessed with a fluorometric plate reader (BIOTEK-FLX800, USA) at excitation and emission wavelengths (green, 485 nm and 535 nm) and (red, 535 nm and 590 nm). The procedure was done based on a previous

study (Elumalai, Gunadharini et al. 2012). Then, the ratio of red to green fluorescence was reported compared to control cells.

### 2.12. Analyzing caspase-3 and caspase-9 activity

Caspase-3 and -9 activities were assessed using the calorimetric assay kits (Abcam, Cambridge, MA, USA) according to the manufacturer's protocols. The samples were read on a microplate reader (SpectraFluor, TECAN, Sunrise, Austria) at 405 nm. The fold-increases in caspase-3 and -9 activity were expressed by comparing the data with the activities of the control samples.

### 2.13. Statistical analysis

Data were reported as mean  $\pm$  SD. Statistical analyses were done using one-way ANOVA using SPSS software.  $P < 0.05$  was expressed to be statistically significant.

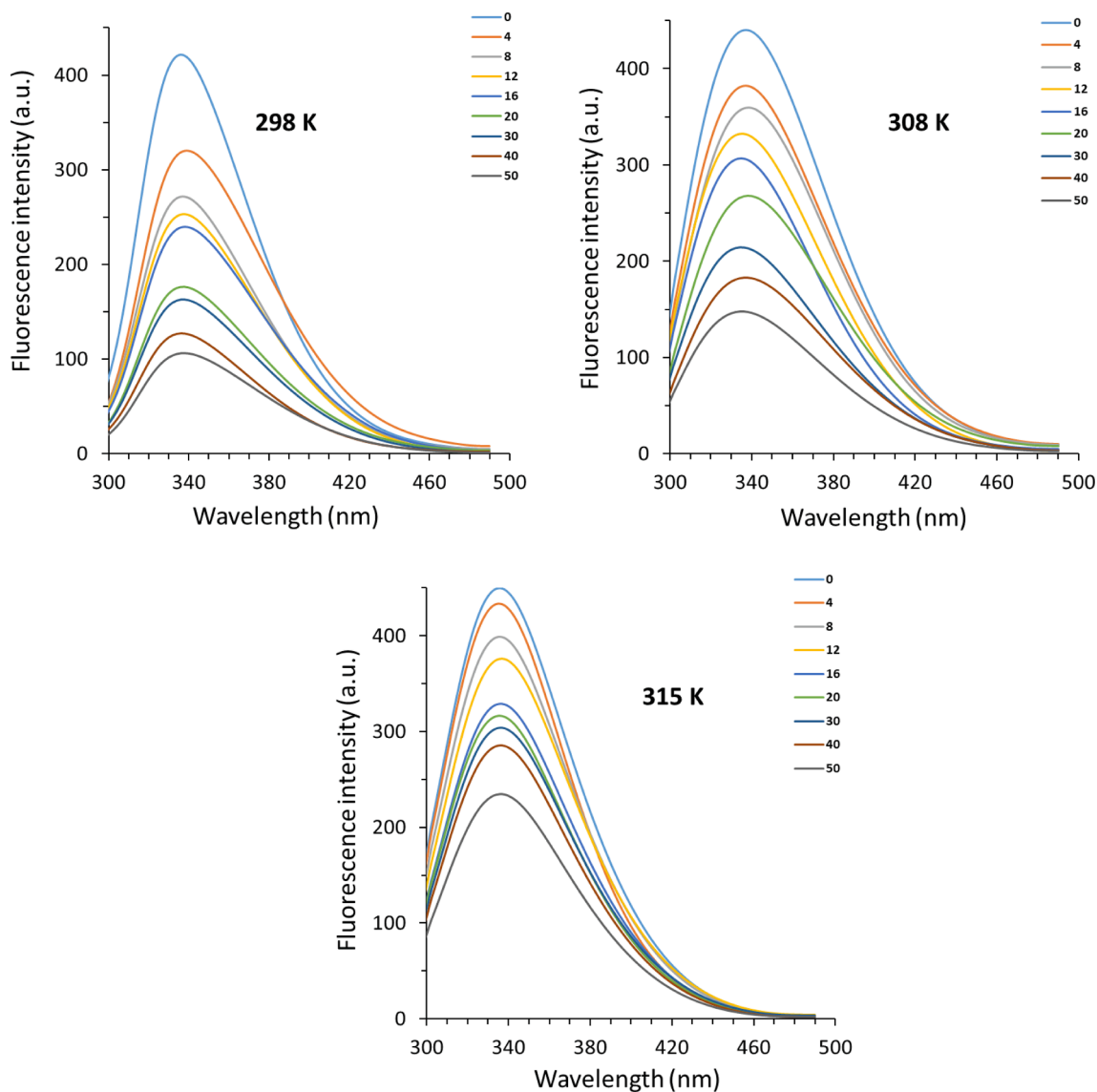


**Fig. 1.** Fluorescence quenching study of hemoglobin with different concentrations of acteoside at three different temperatures. A 3.0 mL solution of hemoglobin (4.00  $\mu M$ ) was added by successive titrations of acteoside with different concentrations varied from 4 to 50  $\mu M$ .

### 3. Results and discussion

#### 3.1. Binding characteristics of acteoside to hemoglobin

Fig. 1 displays the fluorescence spectra of hemoglobin with various concentrations of acteoside. Hemoglobin exhibited a strong fluorescence emission band around 338 nm, when excited at 280 nm. With the addition of acteoside to hemoglobin, the emission intensities of hemoglobin were reduced continuously, indicating that the excited hemoglobin was mainly quenched by acteoside (Kaur, Singh et al. 2023).

Also, no significant wavelength shift toward red or blue was observed, referring to a slight change in the micro-region of tryptophan (Trp) and tyrosine (Tyr) residues (Wang, Zhang et al. 2009b, Patil, Gore et al. 2014) of human hemoglobin following interaction with acteoside.

The resultant fluorescence quenching data (Fig. 1) were analyzed by the Stern–Volmer equation (Eq. (1)) (Farid, Youssef et al. 2023):

$$F_0/F = 1 + K_{SV}[\text{acteoside}] = 1 + k_q\tau_0[\text{acteoside}] \quad (1)$$

where  $F_0$  and  $F$  are known as the fluorescence intensities of hemoglobin in the absence and presence of acteoside, respectively,  $k_q$  and  $K_{SV}$  are the quenching rate constant and the Stern–Volmer quenching constant, respectively,  $\tau_0$  is the average lifetime of protein ( $10^{-8}$  s), and  $[\text{acteoside}]$  is the concentration of ligand (Kaur, Singh et al. 2023). Fig. 2 demonstrates the plots of  $F_0/F$  versus  $[Q]$  of acteoside ranging from 4 to 50  $\mu\text{M}$  (Fig. 2) at 298 K, 308, and 315 K. The plots of hemoglobin-acteoside at three temperatures with good linearity reveal a single quenching mechanism, either static (complex formation between hemoglobin and acteoside) or dynamic (a collisional process between hemoglobin and acteoside) (Quds, Hashmi et al. 2022, Sett, Paul et al. 2022). In other words, a linear Stern–Volmer plot for the interaction of hemoglobin with acteoside reflects either only one acteoside binding site presenting in the vicinity of aromatic residues or more than one binding site on hemoglobin structure with equal accessibility to acteoside (Jin and Zhang, 2008). Linear fittings of the experimental results to Eq. (1) afforded the values of  $K_{SV}$  and  $k_q$  summarized in Table 1.

It was deduced that the values of  $K_{SV}$  decreased with elevating the temperature, indicating that the fluorescence quenching of hemoglobin by acteoside occurs via a static quenching mechanism. Also, the values

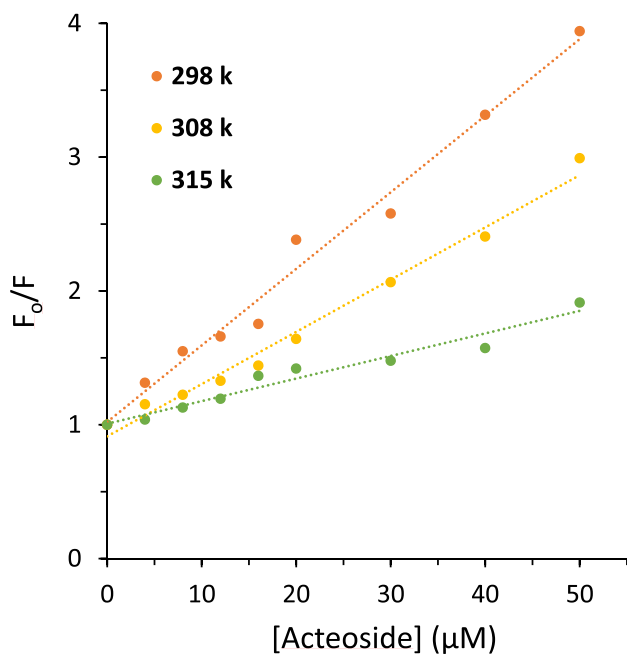


Fig. 2. Stern-Volmer plots derived from the fluorescence quenching study of hemoglobin with different concentrations of acteoside at three temperatures.

Table 1

Quenching constants for human hemoglobin-acteoside system at different temperatures and pH 7.40.

Protein	T (K)	$K_{SV} \times 10^4 (\text{M}^{-1})$	$k_q \times 10^{12} (\text{M}^{-1} \text{s}^{-1})$	$R^a$
Hemoglobin	298	5.72	5.72	0.9840
	308	3.90	3.90	0.9857
	315	1.69	1.69	0.9526

for  $k_q$  in Table 1 stemmed from Eq. (1), are in the magnitude of  $10^{12} \text{ L M}^{-1} \text{ s}^{-1}$ , which are 2 orders of magnitude higher than the maximum diffusion collision quenching rate constant ( $2.0 \times 10^{10} \text{ L mol}^{-1} \text{ s}^{-1}$ ) (Maltas, 2014, Lei, Qin et al. 2022).

Therefore, it was proposed that a static quenching mechanism resulting from a complex formation might be primarily responsible for the fluorescence quenching of hemoglobin by acteoside (Farajzadeh-Dehkordi, Farhadian et al. 2023).

#### 3.2. Analysis of binding equilibria

Based on a static quenching mechanism, ligands could independently interact with a set of equivalent binding sites on a protein (Jin and Zhang, 2008). As a result, an equilibrium between unbound and bound ligands is given by Eq. (2):

$$\log F_0 - F/F = n \log[\text{acteoside}] + \log K_b \quad (2)$$

where  $K_b$  and  $n$  are the binding constant and number of binding sites, respectively which could be calculated by a plot of  $\log(F_0 - F)/F$  vs.  $\log[\text{acteoside}]$ . Plots of  $\log(F_0 - F)/F$  against  $\log[\text{acteoside}]$  (Fig. 2) afforded the values of  $K_b$  and  $n$  tabulated in Table 2. It exhibits that the values of  $K_b$  increase with rising temperature, suggesting the formation of hemoglobin-acteoside complex which its stability is increasing with rising temperature (Salam, Arif et al. 2023). Furthermore, the values of  $n$  were close to one, inferring that there is probably one type of binding site on hemoglobin for acteoside binding (Tian, Zhou et al. 2022, Platanic Arizanović, Gligorijević et al. 2023).

#### 3.3. Determination of the interaction forces

Calculation of thermodynamic parameters following the interaction of small molecules with proteins can provide useful information for the determination of binding parameters. If an enthalpy change ( $\Delta H^0$ ) is almost constant over temperature (T), its value as well as an entropy change ( $\Delta S^0$ ) can be estimated by the van't Hoff Eq. (3):

$$\ln K_b = -\Delta H^0/RT + \Delta S^0/R \quad (3)$$

where  $R$  is the gas constant.

Then, a free energy change ( $\Delta G^0$ ) for a ligand–protein complex can be determined from Eq. (4):

$$\Delta G^0 = \Delta H^0 - T\Delta S^0 \quad (4)$$

The calculated results based on Fig. 3 are collected in Table 3. Fig. 4.

A negative value for  $\Delta G^0$  and a positive value for  $\Delta H^0$  indicated that the formation of hemoglobin-acteoside complex occurred spontaneously through an endothermic process (Maltas and Ozmen, 2015, Chatterjee and Kumar, 2016, Rajendran and Chandrasekaran, 2023). The positive values of  $\Delta H^0$  (75.39 kJ/mol) and  $\Delta S^0$  (333.57 J mol<sup>-1</sup> K<sup>-1</sup>) for

Table 2

Binding parameters for human hemoglobin-acteoside system at different temperatures.

Protein	T (K)	$\log K_b$	$n$	$R^a$
Hemoglobin	298	4.26	0.89	0.9672
	308	4.77	1.05	0.9749
	315	4.96	1.15	0.9498

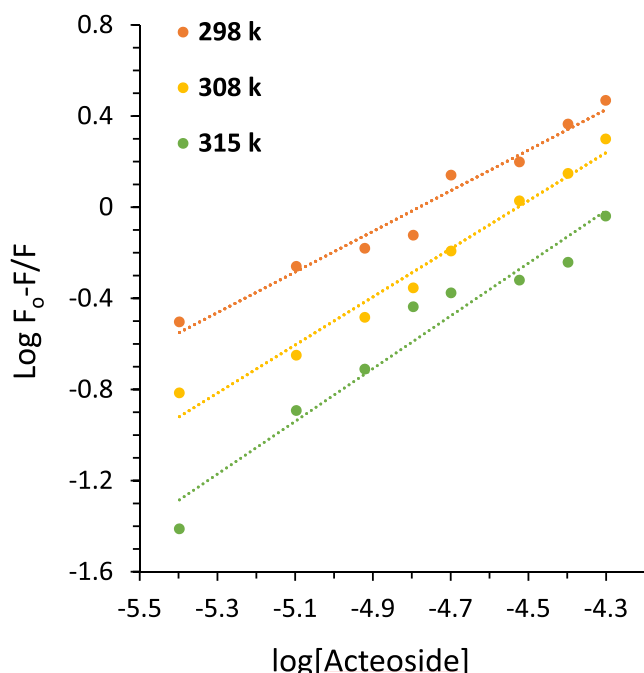


Fig. 3. Modified Stern-Volmer plots derived from fluorescence quenching study of hemoglobin with different concentrations of acteoside at three temperatures.

Table 3

Thermodynamic parameters for human hemoglobin-acteoside system at different temperatures and pH 7.40.

Protein	T (K)	$\Delta H^{\circ}$ (kJ/mol)	$\Delta S^{\circ}$ (J/mol K)	$\Delta G^{\circ}$ (kJ/mol)
Hemoglobin	298			-24.36
	308	75.39	333.57	-27.70
	315			-30.03

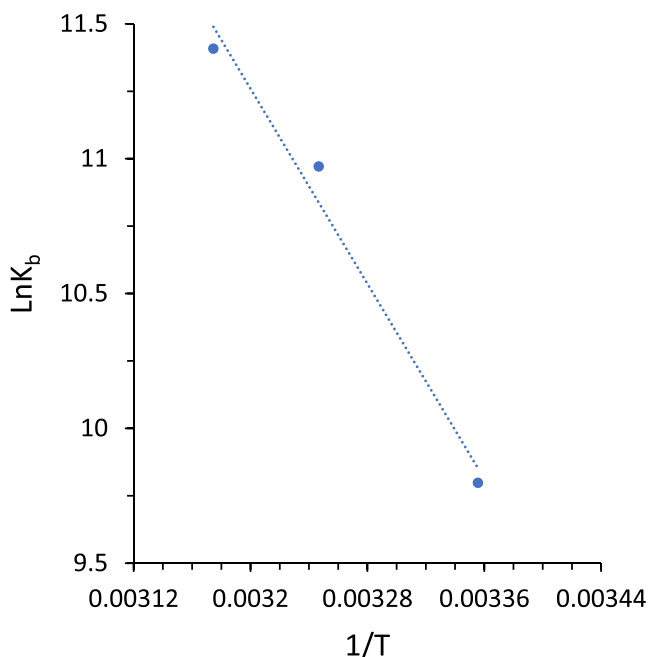


Fig. 4. van't Hoff plot derived from fluorescence quenching study of hemoglobin with different concentrations of acteoside at three temperatures.

hemoglobin-acteoside complex demonstrated that different

intermolecular interactions including hydrophobic, hydrogen bonds, and van der Waals forces are present in this system, while hydrophobic forces might have a dominant contribution. Therefore, hydrophobic forces are assumed to play a key role in the binding of acteoside to hemoglobin (Jiang, Wang et al. 2023).

### 3.4. Molecular docking study

To investigate possible molecular recognition of hemoglobin-acteoside complex, the molecular docking simulation was carried out. Molecular docking analysis provides us with investigating several useful parameters for protein-ligand interactions including binding site, energy, and number of binding sites (Salam, Arif et al. 2023). The acteoside (Fig. 5A) binding site of hemoglobin (Fig. 5B) was surrounded by different amino acid residues including Phe-36 (hydrophobic), Val-96 (hydrophobic), Leu-100 (hydrophobic), Ala-130 (hydrophobic), Thr-38 (hydrogen bond), Asp-99 (hydrogen bond), Glu-101 (hydrogen bond), Arg-104 (hydrogen bond), Asn-108 (hydrogen bond), Gln-131 (hydrogen bond), and Lys-99 (cation- $\pi$ ) (Fig. 5C).

The molecular docking studies showed that acteoside binds in the vicinity of the heme group, indicating that this ligand could interfere with the oxygen-binding site of hemoglobin (Salam, Arif et al. 2023). Also, both hydrophobic and hydrophilic amino acids contribute to the binding of acteoside to hemoglobin. Thus, we can conclude that hydrophobic forces, hydrogen bonding and van der Waals interactions could play a key role in the formation of acteoside-hemoglobin complex. The overall docking energy of acteoside-hemoglobin complex was reported to be  $-9.7$  kcal/mole (40.58 kJ/mol). Interestingly, our experimental outcomes for binding forces correlate well with the theoretical docking simulation, while the calculated binding energies are different, which is a typical discrepancy between theoretical and experimental studies arising from different characteristics of protein and ligands in these measurements.

### 3.5. Protective effect of acteoside on $H_2O_2$ -induced fluorescence quenching of hemoglobin

$H_2O_2$  can stimulate the production of oxidative stress, which can lead to protein structural changes deduced by fluorescence quenching of aromatic amino acid residues (Kosmachevskaya, Nasybullina et al. 2021). Tyr residues, Tyr-42 and Tyr-24, as well as Trp residues, Trp-15 $\beta$  and Trp-37 $\beta$ , are prone to oxidation (Kosmachevskaya, Nasybullina et al. 2021). Therefore, oxidative stress can result in fluorescence quenching of hemoglobin due to the oxidation of aromatic amino acid residues serving as intrinsic fluorophores (Kosmachevskaya, Nasybullina et al. 2021). As a consequence, it was realized that the addition of  $H_2O_2$  to hemoglobin samples results in a significant ( $^{***}P < 0.001$ ) reduction in the fluorescence intensity of hemoglobin, while incubation of samples with acteoside led to a significant ( $^{##}P < 0.01$ ) reduction in fluorescence quenching of hemoglobin triggered by  $H_2O_2$  (Fig. 6).

This data indicated that in the hemoglobin sample, fluorescence intensity was reduced upon incubation with  $H_2O_2$ , revealing oxidation of aromatic residues as well as structural changes of the protein. In the hemoglobin-acteoside, incubated with  $H_2O_2$ , the fluorescence intensity less decreased relative to that of free hemoglobin (Fig. 6), which can be due to the antioxidant characteristics of acteoside.

### 3.6. Structural changes and heme degradation studies

Changes in the secondary and tertiary structure of proteins can be measured by CD spectroscopy (Jia, Buehler et al. 2007, Salam, Arif et al. 2023). The CD spectrum of hemoglobin and hemoglobin-acteoside complex in the absence and presence of  $H_2O_2$  is exhibited in Fig. 7A. The CD spectrum of native hemoglobin showed two negative minima at 209 nm ( $\pi$ - $\pi^*$  transition) and 222 nm ( $n$ - $\pi^*$  transition), corresponding to the dominance of  $\alpha$ -helix structures in protein (Salam, Arif et al. 2023).

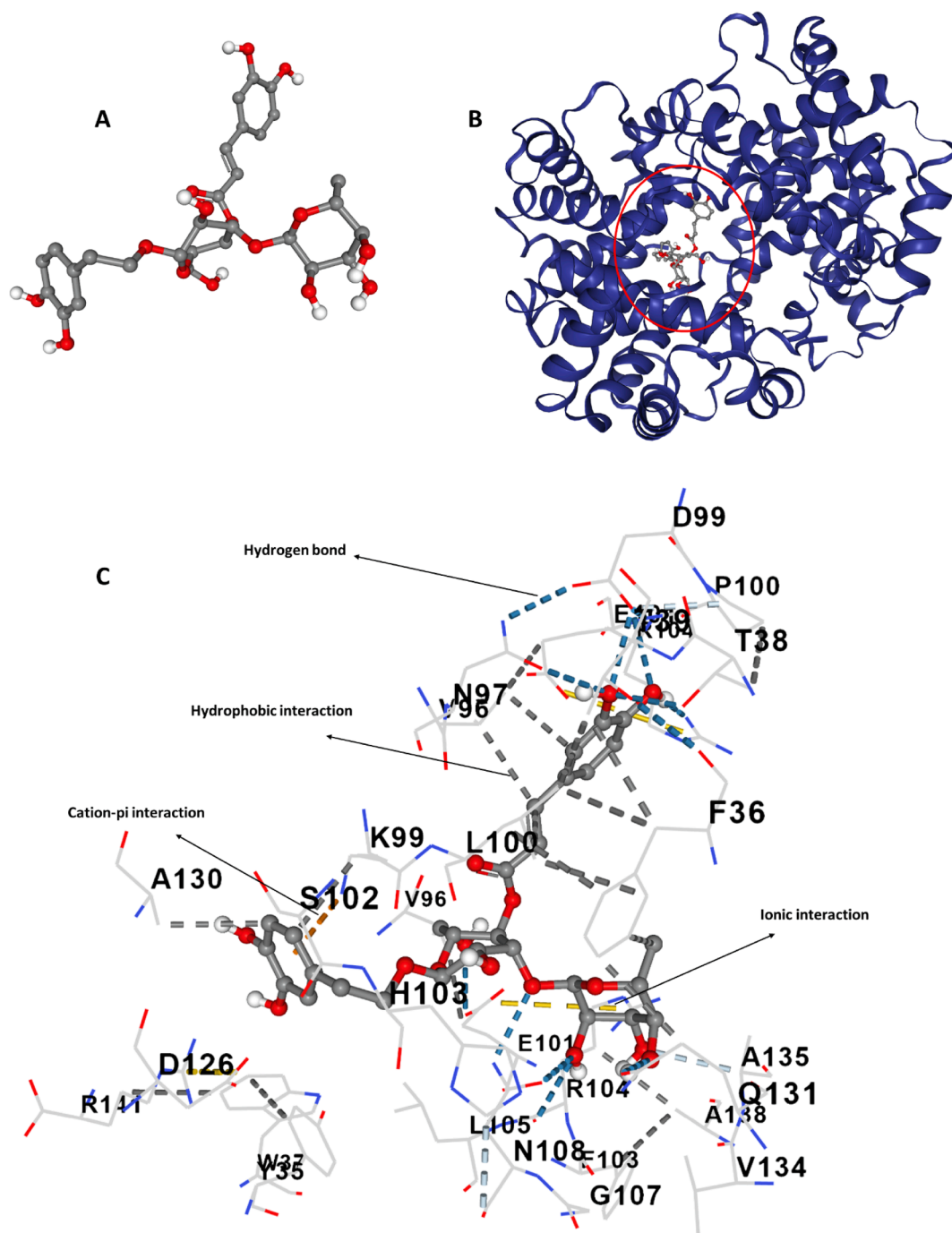
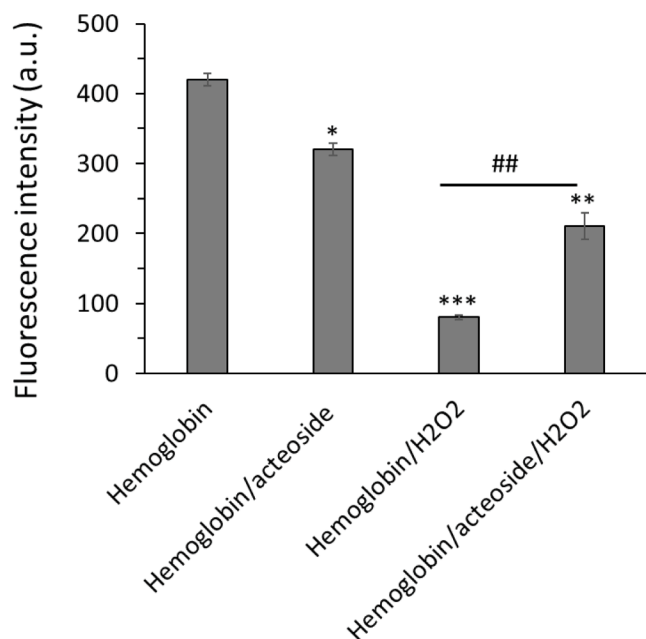


Fig. 5. (A) Structure of acteoside, (B) structure of hemoglobin, (C) amino acid residues in the binding pocket.

In the presence of acteoside, there were no detectable changes in the molar ellipticity values of negative bands of hemoglobin, indicating that the binding of acteoside did not significantly change the secondary structure of hemoglobin. Also, the shape of the CD spectrum of hemoglobin-acteoside remained similar to that of free hemoglobin, revealing the negligible adverse effects of acteoside on hemoglobin structure (Fig. 7A). However, after adding  $H_2O_2$ , the molar ellipticity values of negative bands of hemoglobin were significantly reduced, suggesting a remarkable change in the secondary structure of hemoglobin (Fig. 7A). Interestingly, it was seen that acteoside mitigated the  $H_2O_2$ -induced secondary structural changes of hemoglobin evidenced by lower changes of the molar ellipticity values of hemoglobin relative to those of free hemoglobin.

The percentage of  $\alpha$ -helix in hemoglobin was calculated using CDNN software. It was determined that the  $\alpha$ -helical content decreased from 53.66 % (hemoglobin alone) to 53.12 %, 40.19 % and 45.14 % for hemoglobin-acteoside complex, hemoglobin- $H_2O_2$  and hemoglobin-acteoside- $H_2O_2$ , respectively. The calculated percentage of  $\alpha$ -helical content for free hemoglobin was almost similar to the amount reported previously (Salam, Arif et al. 2023). The decrease in  $\alpha$ -helical structure reveals the less folded secondary structure of hemoglobin in the presence of  $H_2O_2$ , which was recovered upon incubation of protein with acteoside. The CD data indicated that the interaction of acteoside to hemoglobin leads to the hemoglobin backbone adopting a more folded structure following exposure to  $H_2O_2$  which causes less hydrophobic domain exposure to solvent in comparison to free hemoglobin.



**Fig. 6.** Protective effects of acteoside against H<sub>2</sub>O<sub>2</sub>-triggered fluorescence quenching of hemoglobin. The aliquots of hemoglobin (80 μM) incubated with H<sub>2</sub>O<sub>2</sub> (molar ratios of heme to peroxide of 1:5) for 1 h with acteoside (molar ratios of protein to acteoside of 1:1) were withdrawn, diluted to 4 μM and used for protein quenching study. \*\*P < 0.01, \*\*\*P < 0.001 relative to untreated control sample, ##P < 0.01 relative to H<sub>2</sub>O<sub>2</sub>-triggered group.

Furthermore, the impacts of H<sub>2</sub>O<sub>2</sub> treatment and protective effects of acteoside on hemoglobin structure were measured at 420 nm to monitor heme degradation (Jia, Buehler et al. 2007). As depicted in Fig. 7B, the ellipticity changes at 420 nm, corresponding to the integrity of heme groups, reduced upon incubation of hemoglobin with H<sub>2</sub>O<sub>2</sub>, indicating that the structure of the heme groups within the α-helices is significantly changed (Jia, Buehler et al. 2007). However, upon incubation of the hemoglobin-acteoside complex with H<sub>2</sub>O<sub>2</sub>, the ellipticity changes at 420 nm was recovered to some extent relative to free hemoglobin, indicating that oxidation of iron and probable damage to heme groups induced by

H<sub>2</sub>O<sub>2</sub> was alleviated by acteoside (Fig. 7B). Therefore, upon performing the CD experiment in the far-UV region (200–260 nm) and Soret region (420 nm), the data presented in Fig. 7 might indicate that acteoside provided a recovery in the loss of α-helical content and heme group collapse following H<sub>2</sub>O<sub>2</sub> exposure to hemoglobin (Jia, Buehler et al. 2007).

### 3.7. Protective effects of acteoside on H<sub>2</sub>O<sub>2</sub>-induced methemoglobin formation

It has been shown that polyphenols are a great candidate in the regulation of oxidative stress-mediated methemoglobin formation (Blasa, Candiracci et al. 2007, Kong, Mat-Junit et al. 2014, Remigante, Spinelli et al. 2022). Fig. 8 displayed that H<sub>2</sub>O<sub>2</sub> was able to induce the transformation of oxyhemoglobin to methemoglobin. However, acteoside was shown to reduce the formation of methemoglobin stimulated by H<sub>2</sub>O<sub>2</sub>. In fact, the presence of acteoside with promising antioxidant properties results in the attenuation of H<sub>2</sub>O<sub>2</sub>-induced secondary structural changes and heme degradation of hemoglobin as well as the formation of methemoglobin. Thus, the reduction of methemoglobin formation was consistent with the antioxidizing capability of acteoside. In line with our results, Wu et al. reported that plant flavonols could block the formation of methemoglobin and reduced heme degradation which likely derived from the antioxidant capability of quercetin (Wu, Yin et al., 2022b). Furthermore, it has been shown that toxic materials induce adverse effects in human erythrocytes mediated by increased generation of ROS and hemoglobin oxidation (Ahmad and Mahmood, 2019).

### 3.8. Protective effects of acteoside on H<sub>2</sub>O<sub>2</sub>-induced cardiomyocyte toxicity

The H9c2 cells were pretreated with a fixed concentration (10 μM) of acteoside for 12 h followed by washing and treatment with H<sub>2</sub>O<sub>2</sub> (400 μM) for an additional 2 h. As shown in Fig. 9A, acteoside induced no significant damage to cell viability compared with the control group. However, the viability of cells treated with H<sub>2</sub>O<sub>2</sub> (400 μM) for 2 h was reduced significantly (\*\*P < 0.01) in comparison with the control group. The viability of H9c2 cells pretreated with a fixed concentration (10 μM) of acteoside for 12 h before exposure to H<sub>2</sub>O<sub>2</sub> obviously (#P < 0.05)

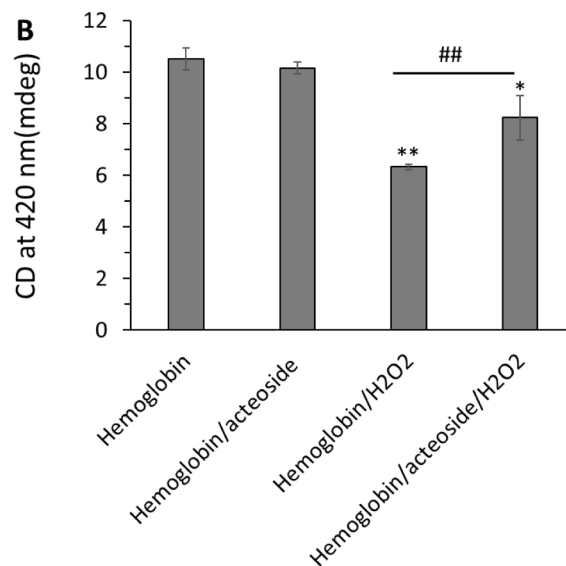
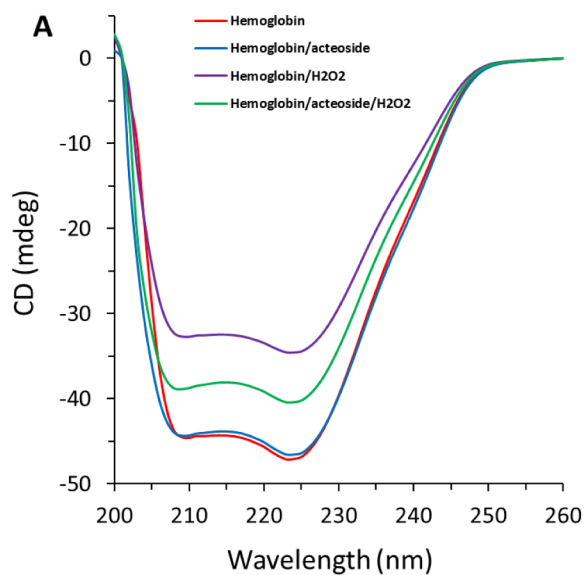


**Fig. 7.** Protective effects of acteoside against H<sub>2</sub>O<sub>2</sub>-triggered (A) secondary structural changes and (B) heme degradation of hemoglobin. The aliquots of hemoglobin (80 μM) incubated with H<sub>2</sub>O<sub>2</sub> (molar ratios of heme to peroxide of 1:5) for 1 h with acteoside (molar ratios of protein to acteoside of 1:1) were withdrawn and used for CD study. \*P < 0.05, \*\*P < 0.01 relative to untreated control sample, ##P < 0.01 relative to H<sub>2</sub>O<sub>2</sub>-triggered group.

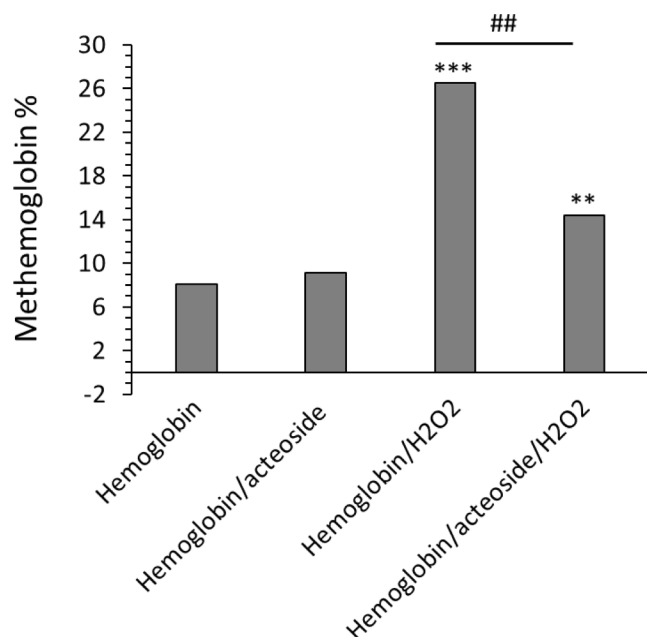


**Fig. 8.** Protective effects of acteoside against H<sub>2</sub>O<sub>2</sub>-triggered methemoglobin formation. The aliquots of hemoglobin (80  $\mu$ M) incubated with H<sub>2</sub>O<sub>2</sub> (molar ratios of heme to peroxide of 1:5) for 1 h with acteoside (molar ratios of protein to acteoside of 1:1) were withdrawn, diluted to 4  $\mu$ M and used for methemoglobin formation detected by UV-Vis study. \*\* $P < 0.01$ , \*\*\* $P < 0.001$  relative to untreated control sample, ## $P < 0.01$  relative to H<sub>2</sub>O<sub>2</sub>-triggered group.

recovered relative to the model group, suggesting the protective effect of acteoside on H9c2 cells on H<sub>2</sub>O<sub>2</sub>-triggered oxidative stress cytotoxicity (Fig. 9A).

It was also shown that acteoside could attenuate the LDH release induced by H<sub>2</sub>O<sub>2</sub> (400  $\mu$ M) in H9c2 cells (Fig. 9B), revealing that acteoside could control the membrane damage in cells triggered by oxidative damage. It was seen that LDH release increased to  $291.28 \pm 25.59$  %, upon incubation of cells with H<sub>2</sub>O<sub>2</sub> (400  $\mu$ M) for 2 h, however, this amount decreased to  $219.31 \pm 3.73$  % (Fig. 9B) in acteoside/H<sub>2</sub>O<sub>2</sub> treated group.

Xi et al. also showed that acteoside (3 mg/ml) could potentially

attenuate H<sub>2</sub>O<sub>2</sub> (400  $\mu$ M)-stimulated injury of retinal ganglion cells (Xi, Ma et al. 2022). Furthermore, several other studies reported that acteoside shows protective effects against oxidative stress triggered by different oxidative molecules such as  $\beta$ -amyloids (Wang, Xu et al., 2009a), free radicals (Chiou, Lin et al. 2004) and *tert*-butyl hydroperoxide (Zhu, Li et al. 2022).

### 3.9. Antioxidant effects of acteoside on H<sub>2</sub>O<sub>2</sub>-induced cardiomyocyte oxidative stress

The protective effects of acteoside against oxidative stress in H9c2 cells were assessed in this study. Fig. 10 shows the levels of lipid peroxidation (MDA), SOD activity, CAT activity, and ROS formation in H9c2 cells treated with acteoside alone (10  $\mu$ M) for 12 h, H<sub>2</sub>O<sub>2</sub> alone (400  $\mu$ M) and their combination.

It was displayed that exposure to H<sub>2</sub>O<sub>2</sub> led to a significant (\*\* $P < 0.001$ ) increase in MDA level in comparison with the control group (Fig. 10A). The pretreatment of acteoside for 12 h followed by the addition of H<sub>2</sub>O<sub>2</sub> decreased significantly ( $\#P < 0.05$ ) this marker (Fig. 10A).

SOD activity was remarkably (\*\* $P < 0.001$ ) decreased to  $47.97 \pm 13.31$  % in H<sub>2</sub>O<sub>2</sub>-treated cells. Acteoside pretreatment significantly ( $\#P < 0.01$ ) increased SOD activity to  $84.16 \pm 16.41$  % (Fig. 10B). CAT activity was substantially (\* $P < 0.05$ ) decreased to  $70.91 \pm 6.62$  % in H<sub>2</sub>O<sub>2</sub>-treated cells., however acteoside pretreatment significantly ( $\#P < 0.05$ ) increased CAT activity to  $88.18 \pm 14.51$  % in cardiomyocyte (Fig. 10C).

Intracellular ROS levels were substantially (\*\* $P < 0.001$ ) elevated to  $347.33 \pm 57.87$  fluorescence units (RFU) in H<sub>2</sub>O<sub>2</sub>-treated cells. However, acteoside pretreatment significantly ( $\#\#\#P < 0.001$ ) reduced the generation of ROS down to  $215.00 \pm 31.48$  RFU in acteoside/H<sub>2</sub>O<sub>2</sub>-treated cells (Fig. 10D).

In agreement with our results, Li et al. (Li, Zhou et al. 2018), Xia et al. (Xia, Zhang et al., 2018), Zhu et al. (Zhu, Li et al. 2022), and Yang et al. (Yang, Hua et al. 2023) reported that acteoside protects different cells against stimulated oxidative stress mediated by regulation of different associated markers such as MDA, SOD, CAT, and ROS.

### 3.10. Protective effects of acteoside on H<sub>2</sub>O<sub>2</sub>-induced mitochondrial damage and apoptosis

Fig. 11 shows the effects of acteoside on MPP, caspase-9 activity, and

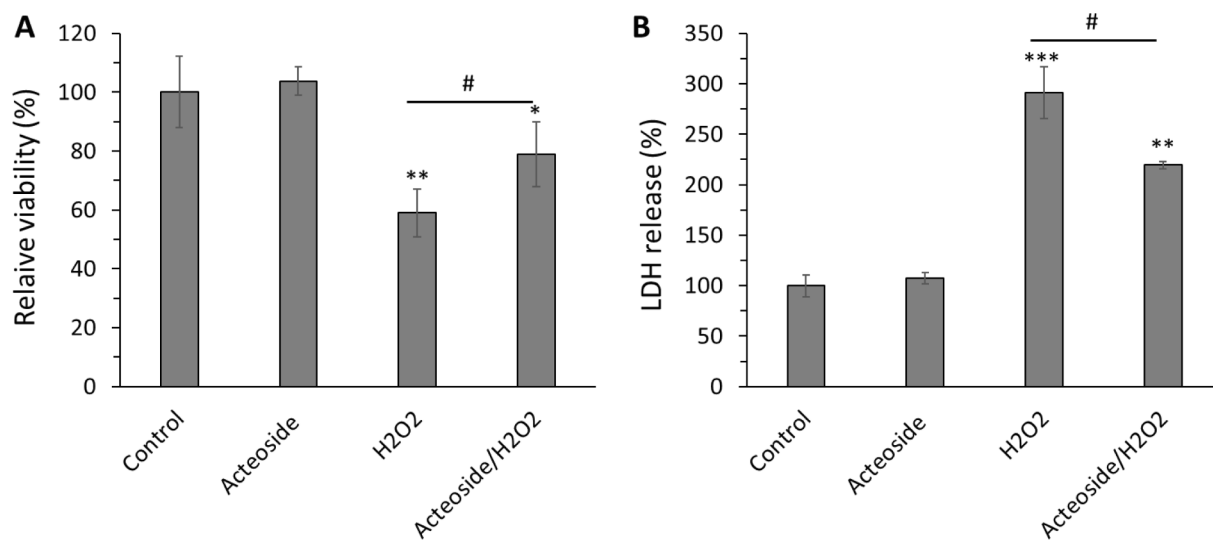


**Fig. 9.** Protective effects of acteoside against H<sub>2</sub>O<sub>2</sub>-triggered cytotoxicity of H9c2 cardiomyocyte cells detected by (A) MTT and (B) LDH release assays. H9c2 cells were pretreated with 10  $\mu$ M of acteoside for 12 h followed by washing and treatment with H<sub>2</sub>O<sub>2</sub> (400  $\mu$ M) for an additional 2 h. Data were presented as mean  $\pm$  SD of three experiments. \* $P < 0.05$ , \*\* $P < 0.01$ , \*\*\* $P < 0.001$  relative to untreated control sample, # $P < 0.05$  relative to H<sub>2</sub>O<sub>2</sub>-triggered group.

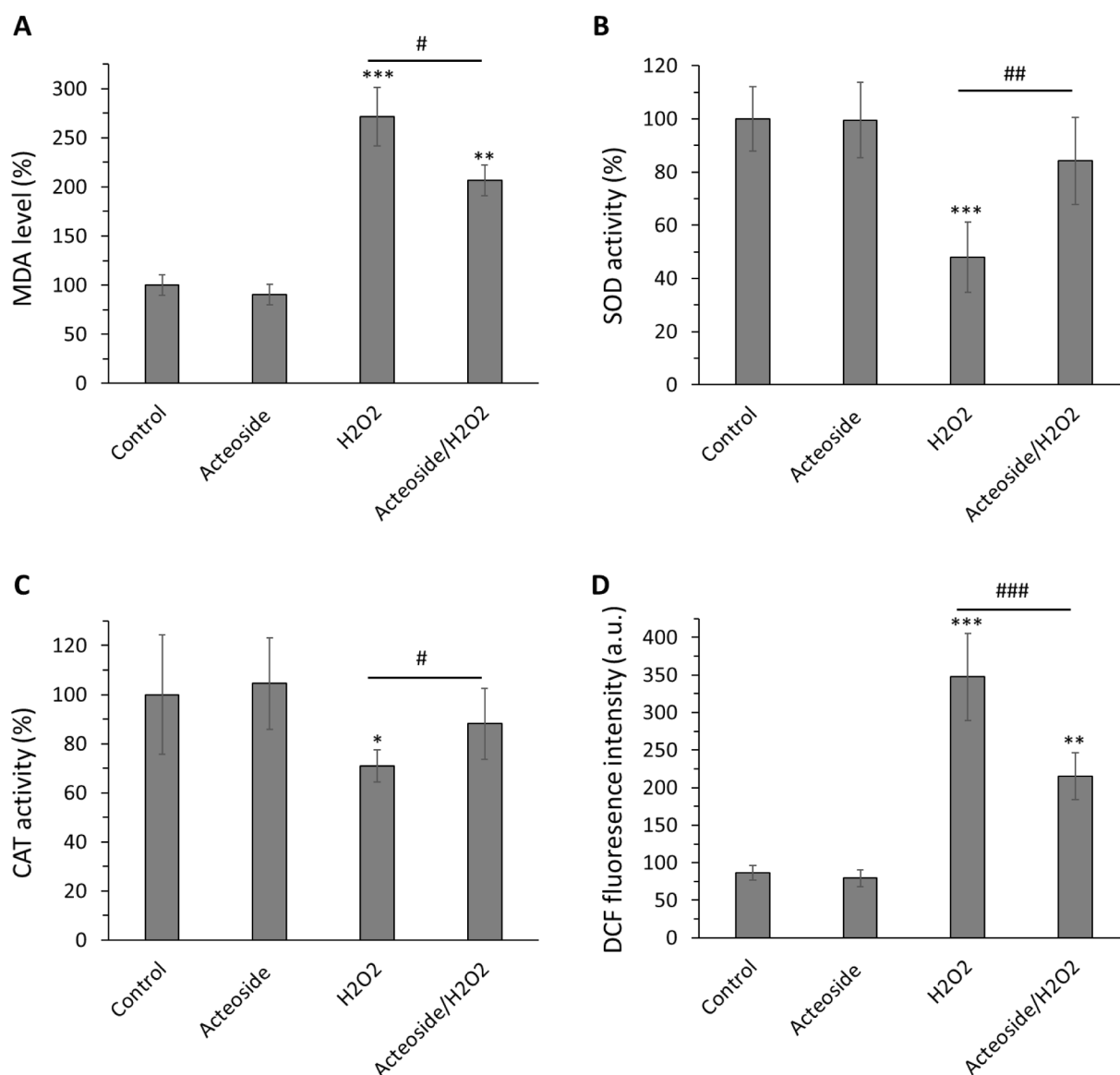


**Fig. 10.** Antioxidant effects of acteoside against H<sub>2</sub>O<sub>2</sub>-triggered oxidative stress in H9c2 cardiomyocyte cells detected by (A) MDA, (B) SOD activity, (C) CAT activity, and (D) ROS assays. H9c2 cells were pretreated with 10  $\mu$ M of acteoside for 12 h followed by washing and treatment with H<sub>2</sub>O<sub>2</sub> (400  $\mu$ M) for an additional 2 h. Data were presented as mean  $\pm$  SD of three experiments. \*P < 0.05, \*\*P < 0.01, \*\*\*P < 0.001 relative to untreated control sample, #P < 0.05, ##P < 0.01, ###P < 0.001 relative to H<sub>2</sub>O<sub>2</sub>-triggered group.

caspase-3 activity levels in H9c2 cells treated with H<sub>2</sub>O<sub>2</sub> alone (400  $\mu$ M). The pretreatment of cells with acteoside alone (10  $\mu$ M) for 12 h maintained the MMP (%) (Fig. 11A), caspase-9 activity (Fig. 11B), and caspase-3 activity (Fig. 11C) almost unchanged to control values. However, treatment with H<sub>2</sub>O<sub>2</sub> alone (400  $\mu$ M) for 2 h resulted in a significant (\*\*P < 0.01) reduction in the percentage of MMP as well as an obvious (\*\*\*) increase of caspase-9 and caspase-3 activity in H9c2 cells. Interestingly, it was detected that acteoside pretreatment prevented these adverse effects observed in H9c2 cells treated with H<sub>2</sub>O<sub>2</sub>.

This study assessed the protective effect of acteoside against oxidative stress and apoptosis in H9c2 cells incubated with H<sub>2</sub>O<sub>2</sub>. Acteoside supplementation has been demonstrated to remarkably mitigate apoptosis in oxidative stress-induced cell models (Lee, Woo et al. 2004, Zhu, Li et al. 2022). For example, it has been reported that acteoside could modulate neurotoxin-stimulated neural oxidative stress and apoptosis mediated by Nrf2-ARE signaling pathway (Li, Zhou et al. 2018). Wu et al. also reported that acteoside shows protective effects against cerebral ischemia/reperfusion damage through regulating

oxidative stress and apoptosis (Wu, Wu et al., 2021). Recently, Cui et al. reported that acteoside could alleviate asthma by regulating oxidative stress-responsive NF- $\kappa$ B signaling pathway (Cui, Tang et al. 2023). We also showed that acteoside could mitigate oxidative stress-induced cardiomyocyte toxicity through the regulation of mitochondrial-mediated apoptosis, evidenced by the recovery of MMP and decrease of caspase-9 and caspase-3 activities.

In general, it should be noted that most antioxidant with phenolic-based structure could undergo multiple mechanisms (e.g., hydrogen-atom-transfer or electron-transfer) to exert the antioxidant and protective action (Ayoubi-Chianeh and Kassae 2020).

#### 4. Conclusion

The present study aimed to study, for the first time, the interaction of acteoside with hemoglobin as well as the protective effects of acteoside on oxidative stress-induced structural changes, heme degradation, and methemoglobin formation *in vitro*. Also, the protective effects of acteoside on H<sub>2</sub>O<sub>2</sub>-induced cytotoxicity, oxidative stress, and apoptosis in

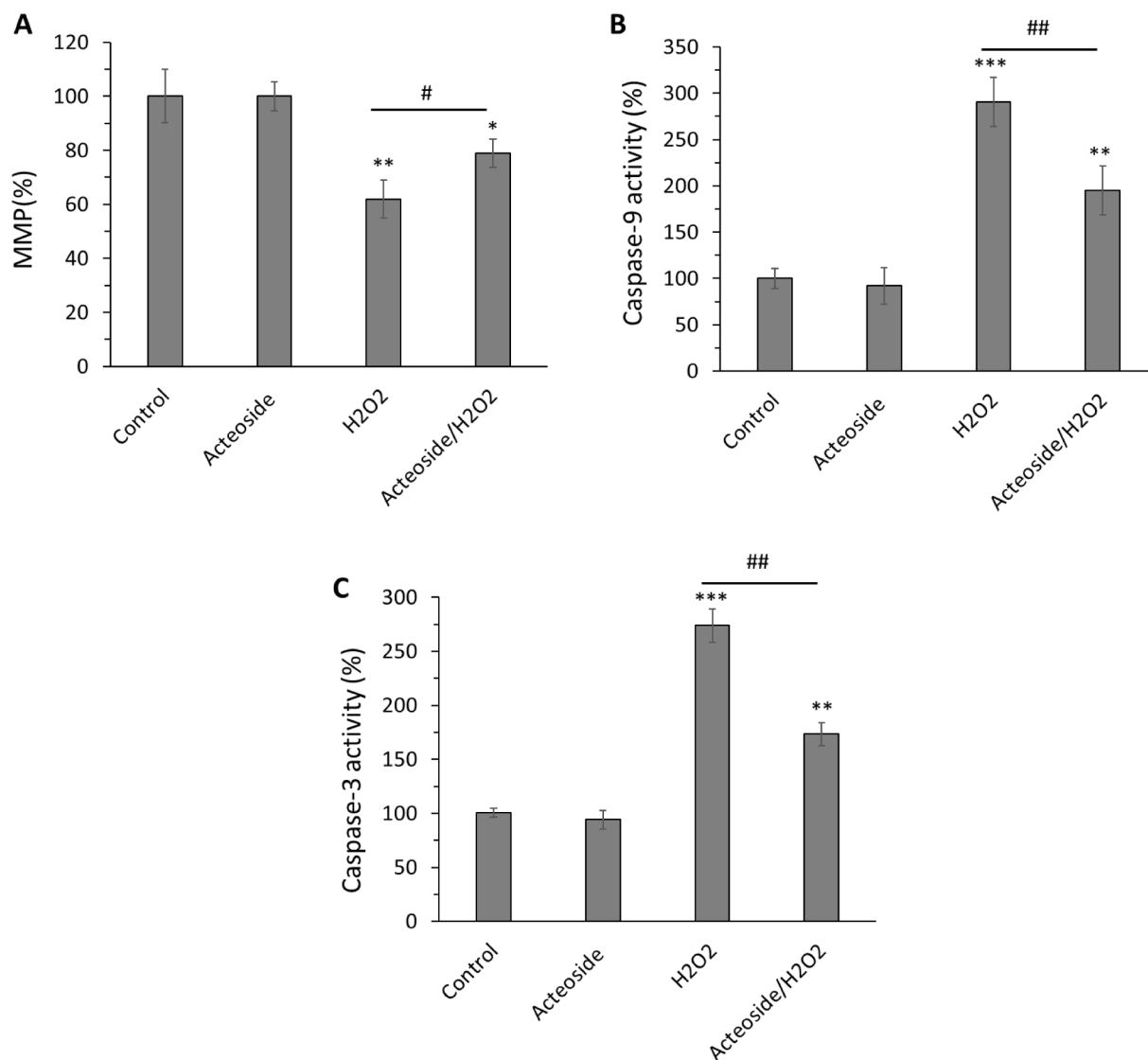


**Fig. 11.** Antiapoptotic effects of acteoside against H<sub>2</sub>O<sub>2</sub>-triggered apoptosis in H9c2 cardiomyocyte cells detected by (A) MMP, (B) caspase-9 activity and (C) caspase-3 activity assays, H9c2 cells were pretreated with 10  $\mu$ M of acteoside for 12 h followed by washing and treatment with H<sub>2</sub>O<sub>2</sub> (400  $\mu$ M) for an additional 2 h. Data were presented as mean  $\pm$  SD of three experiments. \*P < 0.05, \*\*P < 0.01, \*\*\*P < 0.001 relative to untreated control sample, #P < 0.05, ##P < 0.01, relative to H<sub>2</sub>O<sub>2</sub>-triggered group.

H9c2 cardiomyocytes were evaluated. The results presented in this study could be utilized as the basis to evaluate chemical and conformational changes of hemoglobins upon interaction with oxidants as well as bioactive antioxidant compounds. Acteoside also could contribute to the development of potential agents against cytotoxicity, oxidative stress, and apoptosis in cardiomyocyte.

#### Declaration of competing interest

The authors declare that they have no known competing financial interests or personal relationships that could have appeared to influence the work reported in this paper.

#### Acknowledgment

The present work was supported by no external funding.

#### References

Ahmad, S., Mahmood, R., 2019. Mercury chloride toxicity in human erythrocytes: enhanced generation of ROS and RNS, hemoglobin oxidation, impaired antioxidant

power, and inhibition of plasma membrane redox system. *Environ. Sci. Pollut. Res.* 26, 5645–5657.

Ayoubi-Chianeh, M., Kassaee, M.Z., 2020. Novel silylphenol antioxidants by density functional theory. *J. Chin. Chem. Soc.* 67 (11), 1986–1991.

Basu, A., Kumar, G.S., 2016. Multispectroscopic and calorimetric studies on the binding of the food colorant tartrazine with human hemoglobin. *J. Hazard. Mater.* 318, 468–476.

Benesch, R.E., Benesch, R., Yung, S., 1973. Equations for the spectrophotometric analysis of hemoglobin mixtures. *Anal. Biochem.* 55 (1), 245–248.

Blasa, M., Candiracci, M., Accorsi, A., Piacentini, M.P., Piatti, E., 2007. Honey flavonoids as protection agents against oxidative damage to human red blood cells. *Food Chem.* 104 (4), 1635–1640.

Chatterjee, S., Kumar, G.S., 2016. Binding of fluorescent acridine dyes acridine orange and 9-aminoacridine to hemoglobin: Elucidation of their molecular recognition by spectroscopy, calorimetry and molecular modeling techniques. *J. Photochem. Photobiol. B Biol.* 159, 169–178.

Chiou, W.F., Lin, L.C., Chen, C.F., 2004. Acteoside protects endothelial cells against free radical-induced oxidative stress. *J. Pharm. Pharmacol.* 56 (6), 743–748.

Cui, J., Tang, W., Wang, W., Yi, L., Teng, F., Xu, F., Li, M., Ma, M., Dong, J., 2023. Acteoside alleviates asthma by modulating ROS-responsive NF- $\kappa$ B/MAPK signaling pathway. *Int. Immunopharmacol.* 116, 109806.

de Araújo, R. F. F., D. B. G. Martins and M. A. C. S. M. Borba (2016). Oxidative stress and disease. A master regulator of oxidative stress-the transcription factor nrf2, IntechOpen.

Elumalai, P., Gunadharini, D., Senthikumar, K., Banudevi, S., Arunkumar, R., Benson, C., Sharmila, G., Arunakaran, J., 2012. Induction of apoptosis in human

- breast cancer cells by nimbolide through extrinsic and intrinsic pathway. *Toxicol. Lett.* 215 (2), 131–142.
- Farajzadeh-Dehkordi, N., Farhadian, S., Zahraei, Z., Asgharzadeh, S., Shareghi, B., Shakerian, B., 2023. Insights into the binding interaction of Reactive Yellow 145 with human serum albumin from a biophysics point of view. *J. Mol. Liq.* 369, 120800.
- Farid, N.A., Yousef, N.F., Abdellatif, H.E., Sharaf, Y.A., 2023. Spectrofluorimetric methods for the determination of mirabegron by quenching tyrosine and L-tryptophan fluorophores: Recognition of quenching mechanism by Stern-Volmer relationship, evaluation of binding constants and binding sites. *Spectrochim. Acta A Mol. Biomol. Spectrosc.* 293, 122473.
- Jia, Y., Buehler, P.W., Boykins, R.A., Venable, R.M., Alayash, A.I., 2007. Structural basis of peroxide-mediated changes in human hemoglobin: a novel oxidative pathway. *J. Biol. Chem.* 282 (7), 4894–4907.
- Jiang, S.-L., Wang, W.-J., Hu, Z.-Y., Zhang, R.-J., Shi, J.-H., 2023. Comprehending the intermolecular interaction of JAK inhibitor fedratinib with bovine serum albumin (BSA)/human alpha-1-acid glycoprotein (HAG): Multispectral methodologies and molecular simulation. *Spectrochim. Acta A Mol. Biomol. Spectrosc.* 123277.
- Jin, J., Zhang, X., 2008. Spectrophotometric studies on the interaction between pazufloxacin mesilate and human serum albumin or lysozyme. *J. Lumin.* 128 (1), 81–86.
- Kaur, L., Singh, A., Datta, A., Ojha, H., 2023. Multispectroscopic studies of binding interaction of phosmet with bovine hemoglobin. *Spectrochim. Acta A Mol. Biomol. Spectrosc.* 296, 122630.
- Kong, K.W., Mat-Junit, S., Ismail, A., Aminudin, N., Abdul-Aziz, A., 2014. Polyphenols in *Barringtonia racemosa* and their protection against oxidation of LDL, serum and haemoglobin. *Food Chem.* 146, 85–93.
- Kosmachevskaya, O.V., Nasybullina, E.I., Shumaev, K.B., Novikova, N.N., Topunov, A.F., 2021. Protective effect of dinitrosyl iron complexes bound with hemoglobin on oxidative modification by peroxynitrite. *Int. J. Mol. Sci.* 22 (24), 13649.
- Lee, K.J., Woo, E.-R., Choi, C.Y., Shin, D.W., Lee, D.G., You, H.J., Jeong, H.G., 2004. Protective effect of acteoside on carbon tetrachloride-induced hepatotoxicity. *Life Sci.* 74 (8), 1051–1064.
- Lei, X., Qin, Z., Ye, B., Guo, F., Wu, Y., Liu, L., 2022. Interaction between secondary lipid oxidation products and hemoglobin with multi-spectroscopic techniques and docking studies. *Food Chem.* 394, 133497.
- Li, M., Zhou, F., Xu, T., Song, H., Lu, B., 2018. Acteoside protects against 6-OHDA-induced dopaminergic neuron damage via Nrf2-ARE signaling pathway. *Food Chem. Toxicol.* 119, 6–13.
- Liguori, I., G. Russo, F. Curcio, G. Bulli, L. Aran, D. Della-Morte, G. Gargiulo, G. Testa, F. Cacciatore and D. Bonaduce (2018). "Oxidative stress, aging, and diseases." *Clinical interventions in aging: 757-772*.
- Maltas, E., Ozmen, M., 2015. Spectrofluorometric and thermal gravimetric study on binding interaction of thiabendazole with hemoglobin on epoxy-functionalized magnetic nanoparticles. *Mater. Sci. Eng. C* 54, 43–49.
- Maltas, E. (2014). "Binding interactions of niclosamide with serum proteins." *Journal of food and drug analysis* 22(4): 549-555.
- Patil, M.V., Gore, A.H., Lee, S.H., Anbhule, P.V., Patil, S.R., Kolekar, G.B., 2014. Comparative Spectroscopic Studies on Binding Interaction of Theophylline with Human Hemoglobin: Mechanistic and Conformational Investigations. *Int. J. Sci. Technol.* 2 (12), 202.
- Platanić Arizanović, L., Gligorićević, N., Cvijetić, I., Mijatović, A., Ristivojević, M.K., Minić, S., Kokić, A.N., Miljević, Č., Nikolić, M., 2023. Human Hemoglobin and Antipsychotics Clozapine, Ziprasidone and Sertindole: Friends or Foes? *Int. J. Mol. Sci.* 24 (10), 8921.
- Quds, R., Hashmi, M.A., Iqbal, Z., Mahmood, R., 2022. Interaction of mancozeb with human hemoglobin: Spectroscopic, molecular docking and molecular dynamic simulation studies. *Spectrochim. Acta A Mol. Biomol. Spectrosc.* 280, 121503.
- Rajendran, D., Chandrasekaran, N., 2023. Molecular Interaction of Functionalized Nanoplastics with Human Hemoglobin. *J. Fluoresc.* 1–16.
- Rasheed, Z., Alharbi, A., Alrakebeh, A., Almansour, K., Almadi, A., Almuzaini, A., Salem, M., Aloboody, B., Alkobair, A., Albegami, A., 2022. Thymoquinone provides structural protection of human hemoglobin against oxidative damage: Biochemical studies. *Biochimie* 192, 102–110.
- Reeder, B.J., Wilson, M.T., 2005. Hemoglobin and myoglobin associated oxidative stress: from molecular mechanisms to disease states. *Curr. Med. Chem.* 12 (23), 2741–2751.
- Remigante, A., Morabito, R., 2022. Cellular and molecular mechanisms in oxidative stress-related diseases. *MDPI* 23, 8017.
- Remigante, A., Spinelli, S., Straface, E., Gambardella, L., Caruso, D., Falliti, G., Dossena, S., Marino, A., Morabito, R., 2022. Antioxidant activity of quercetin in a H2O2-induced oxidative stress model in red blood cells: Functional role of Band 3 protein. *Int. J. Mol. Sci.* 23 (19), 10991.
- Salam, S., Arif, A., Nabi, F., Mahmood, R., 2023. Molecular docking and biophysical studies on the interaction between thiram and human hemoglobin. *J. Mol. Struct.* 1272, 134188.
- Sett, R., Paul, B.K., Guchhait, N., 2022. Deciphering the fluorescence quenching mechanism of a flavonoid drug following interaction with human hemoglobin. *J. Phys. Org. Chem.* 35 (3), e4307.
- Shi, P., Geng, Q., Chen, L., Du, T., Lin, Y., Lai, R., Meng, F., Wu, Z., Miao, X., Yao, H., 2020. Schisandra chinensis bee pollen's chemical profiles and protective effect against H2O2-induced apoptosis in H9c2 cardiomyocytes. *BMC Complem. Med. Therap.* 20 (1), 1–14.
- Tian, R., Zhou, L., Lu, N., 2022. Binding of quercetin to hemoglobin reduced heme release and lipid oxidation. *J. Agric. Food Chem.* 70 (40), 12925–12934.
- Wang, H., Xu, Y., Yan, J., Zhao, X., Sun, X., Zhang, Y., Guo, J., Zhu, C., 2009a. Acteoside protects human neuroblastoma SH-SY5Y cells against  $\beta$ -amyloid-induced cell injury. *Brain Res.* 1283, 139–147.
- Wang, Y.-Q., Zhang, H.-M., Zhou, Q.-H., 2009b. Studies on the interaction of caffeine with bovine hemoglobin. *Eur. J. Med. Chem.* 44 (5), 2100–2105.
- Wu, H., Guo, J., Yao, Y., Xu, S., 2022a. Polystyrene nanoplastics induced cardiomyocyte apoptosis and myocardial inflammation in carp by promoting ROS production. *Fish Shellfish Immunol.* 125, 1–8.
- Wu, W., Wu, G., Cao, D., 2021. Acteoside presents protective effects on cerebral ischemia/reperfusion injury through targeting CCL2, CXCL10, and ICAM1. *Cell Biochem. Biophys.* 79, 301–310.
- Wu, H., Yin, J., Xiao, S., Zhang, J., Richards, M.P., 2022b. Quercetin as an inhibitor of hemoglobin-mediated lipid oxidation: Mechanisms of action and use of molecular docking. *Food Chem.* 384, 132473.
- Xi, X., Ma, J., Chen, Q., Wang, X., Xia, Y., Wen, X., Yuan, J., Li, Y., 2022. Acteoside attenuates hydrogen peroxide-induced injury of retinal ganglion cells via the CAS2/miR-155/mTOR axis. *Annals of Translational Medicine* 10 (1).
- Xia, D., Zhang, Z., Zhao, Y., 2018. Acteoside attenuates oxidative stress and neuronal apoptosis in rats with focal cerebral ischemia-reperfusion injury. *Biol. Pharm. Bull.* 41 (11), 1645–1651.
- Xiao, Y., Ren, Q., Wu, L., 2022. The pharmacokinetic property and pharmacological activity of acteoside: A review. *Biomed. Pharmacother.* 153, 113296.
- Yang, J., Hua, Z., Zheng, Z., Ma, X., Zhu, L., Li, Y., 2023. Acteoside inhibits high glucose-induced oxidative stress injury in RPE cells and the outer retina through the Keap1/Nrf2/ARE pathway. *Exp. Eye Res.* 109496.
- Zhang, D., Li, Y., Heims-Waldron, D., Bezzerides, V., Guatimosin, S., Guo, Y., Gu, F., Zhou, P., Lin, Z., Ma, Q., 2018. Mitochondrial cardiomyopathy caused by elevated reactive oxygen species and impaired cardiomyocyte proliferation. *Circ. Res.* 122 (1), 74–87.
- Zhu, J., Li, G., Zhou, J., Xu, Z., Xu, J., 2022. Cytoprotective effects and antioxidant activities of acteoside and various extracts of *Clerodendrum cyrtophyllum* Turcz leaves against t-BHP induced oxidative damage. *Sci. Rep.* 12 (1), 12630.